

EMISSION OF HIGH ENERGY PARTICLES IN HEAVY ION COLLISIONS AND A NON-EQUILIBRIUM EQUATION OF STATE

A.T. D'yachenko¹, I.A. Mitropolsky²

¹Emperor Alexander I Petersburg State Transport University;

²NRC "Kurchatov Institute",

B.P. Konstantinov Petersburg Nuclear Physics Institute

A hydrodynamic approach with a non-equilibrium equation of state is used to describe the collision dynamics of heavy ions of medium and intermediate energies. In the development of this approach, with the inclusion of nuclear viscosity effects and the introduction of an amendment to the microcanonical distribution, the double differential cross sections of proton emission in collisions of different nuclei are calculated, which are in agreement with the available experimental data on the emission of high-energy particles, including the cumulative spectral region.

Ядро-снаряд

Спектаторы снаряда

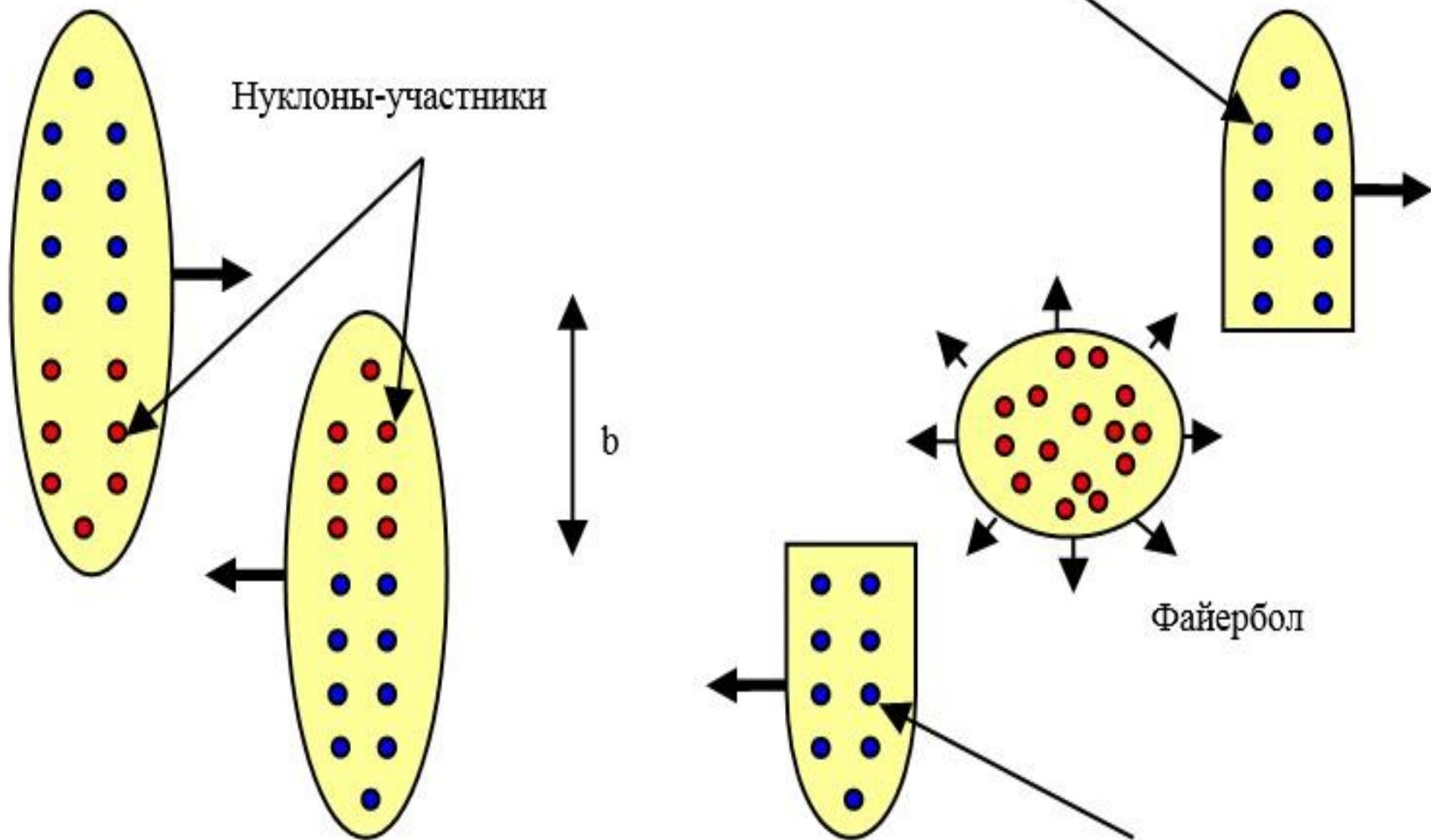
Нуклоны-участники

b

Файербол

Ядро-мишень

Спектаторы мишени



1. THE EQUATIONS OF A NON-EQUILIBRIUM HYDRODYNAMICS

- To describe the collisions of heavy ions we use the non-equilibrium hydrodynamic approach [1,2,3,4], in which the kinetic equation for the nucleon distribution function is solved jointly with the equations of hydrodynamics, which are essentially local laws of conservation of mass, momentum and energy. $\int \frac{d^3\vec{p}}{(2\pi\hbar)^3} \quad 1, \vec{p}, p^2$

$$\frac{\partial f}{\partial t} + \frac{p_i}{m} \frac{\partial f}{\partial x_i} - \frac{\partial W}{\partial x_i} \frac{\partial f}{\partial p_i} = \frac{f_0 - f}{\tau}, \quad (1)$$

$$\frac{\partial \rho}{\partial t} + \frac{\partial}{\partial x_i} (\rho v_i) = 0, \quad (2)$$

$$\frac{\partial}{\partial t} (m\rho v_i) + \frac{\partial}{\partial x_j} (m\rho v_i v_j + P_{ij}) = 0$$

$$\frac{\partial}{\partial t} (m\rho v^2 / 2 + e) + \frac{\partial}{\partial x_j} (v_j (m\rho v^2 / 2 + e) + v_i P_{ij}) = 0$$

- $\rho = \int \frac{fd^3\vec{p}}{(2\pi\hbar)^3} \quad \tau = \lambda / v_T \quad W(\rho) = \alpha\rho + \beta\rho^\gamma,$
- $f(\vec{r}, \vec{p}, t) = f_1 \cdot q + f_0 \cdot (1 - q)$

(3)

- $P_{kin}^{\parallel} = P_{(kin)11} = 2(\varepsilon_1 + I_1)q + \frac{2}{3}(\varepsilon + I)(1 - q) \quad \varepsilon_1 = \frac{\hbar^2}{10m} \left(\frac{3}{2} \pi^2 \rho_0 \right)^{2/3} \frac{\rho^3}{\rho_0^2}$

- $P_{kin}^{\perp} = P_{(kin)22} = P_{(kin)33} = 2\varepsilon_2 + \frac{2}{3}(\varepsilon + I)(1 - q) \quad \varepsilon_2 = \frac{\hbar^2}{10m} \left(\frac{3}{2} \pi^2 \rho_0 \right)^{2/3} \rho$

- $\varepsilon = \frac{3}{10} \frac{\hbar^2}{m} \left(\frac{3}{2} \pi^2 \rho \right)^{2/3} \cdot \rho \quad I = \int \frac{p^2}{2m} \delta f \frac{d^3\vec{p}}{(2\pi\hbar)^3} \quad I_1 = \int \frac{p^2}{2m} \delta f_1 \frac{d^3\vec{p}}{(2\pi\hbar)^3}$

- $P_{ij} = P_{(kin)ij} + P_{int} \delta_{ij} \quad e = \varepsilon + I + e_{int} \quad e_{int} = \int_0^{\rho} W(\rho) d\rho \quad P_{int} = \rho^2 \frac{d(e_{int} / \rho)}{d\rho}$
- $\frac{\partial}{\partial t} ((\varepsilon_1 - \varepsilon_2 + I_1)q) + \frac{\partial}{\partial x_1} (v_1(3\varepsilon_1 - \varepsilon_2 + 3I_1)q) + \sum_{i=2,3} \frac{\partial}{\partial x_i} (v_i(\varepsilon_1 - \varepsilon_2 + I_1)q) +$

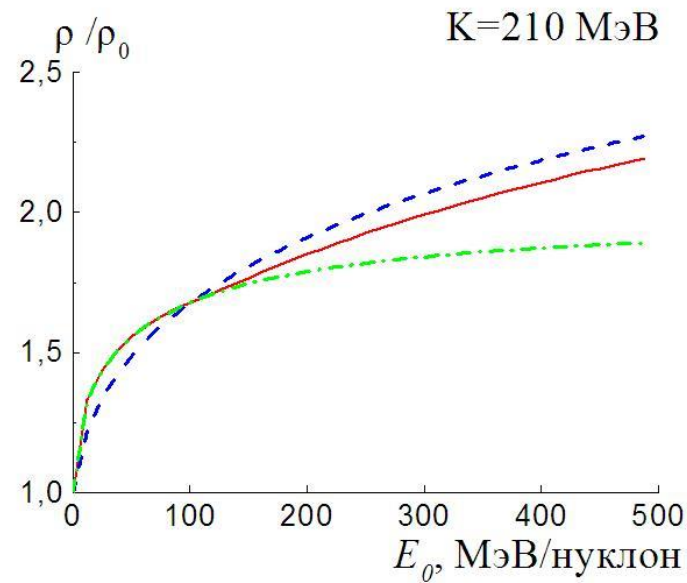
- $\rho v_1 \frac{\partial W}{\partial x_1} - \sum_{i=2,3} \frac{\rho v_i}{2} \frac{\partial W}{\partial x_i} = - \frac{(\varepsilon_1 - \varepsilon_2 + I_1)q}{\tau}$

(4)

$$p_1^2 - (p_2^2 + p_3^2) / 2$$

2.THE HYDRODYNAMIC STAGE

- After selecting the region of the local heating, hot spot - the overlap region of the colliding nuclei, we analyze the stages of compression, expansion and freeze-out of matter during the collision of heavy ions. At the compression stage, a collisionless shock wave with a changing front is formed [2]. At the expansion stage [3], when the shock wave reaches the boundaries of hot spot, the initially compressed system is expanded, we describe it in the relaxation approximation taking into account the nuclear viscosity [4]. As the relaxation time we take $\tau = \lambda / v_T$, where $\lambda = 1 / \sigma \rho$ is the mean free path, $\sigma \approx 40 \text{mb}$ is the total nucleon-nucleon cross section, ρ is the nucleon density, and v_T is the average velocity of the thermal motion of the nucleons. At the freeze-out stage, when the system reaches a critical density also called the freeze-out density, the system does not "hold itself" and the secondary particles are formed [1, 2, 3, 4, 5].



- Fig. 1. Dependence on the collision energy of the maximum compression ratio
- ρ/ρ_0 achieved in the central collision of nuclei for the case of the relaxation factor
- q (solid line) calculated by us, for the case when the factor $q=0$
- (dashed line), and for the case when $q=1$ (a dashed-dot line)

3. A COMPARISON WITH EXPERIMENTAL DATA

- As a result, the double differential cross-section of proton emission has the form (where b is the impact parameter, \hbar is a Planck constant, \vec{r} is the radius vector):

$$\frac{d^2\sigma}{dEd\Omega} = \frac{2\pi}{(2\pi\hbar)^3} \int G(b) b db d\vec{r} \gamma(E - \vec{p}\vec{v}) p f(\vec{r}, \vec{p}, t) \quad (5)$$

- where the distribution function of emitted protons

$$f(\vec{r}, \vec{p}, t) = g \left[\exp\left(\frac{\gamma(E - \vec{p}\vec{v}) - \mu + T\delta}{T}\right) + 1 \right]^{-1} \quad (6)$$

- Here the spin factor $g = 2$, $E = \sqrt{p^2 + m^2}$, γ and \vec{p} are respectively the total energy, the Lorentz factor and the proton momentum; $\vec{v}(\vec{r}, t)$ is the velocity field, $G(b)$ is the factor taking into account that the cross section of the hot spot formation is always greater than the geometric one, μ is the chemical potential, which is found from the conservation of the average number of particles for a grand canonical ensemble, T is the temperature, δ is correction for the microcanonical distribution, which for the kinetic energy $\varepsilon = E - m > E_1$ is equal to

$$\delta = \left[M \ln \left(1 - \frac{\gamma(E - \vec{p}\vec{v}) - m}{MT} \right) - \frac{\gamma(E - \vec{p}\vec{v}) - m}{T} \right] \quad (7)$$

where $M = 3N / 2$, N is the number of nucleons in the thermostat, $E_1 (E_1 \gg T)$ is the energy that is close to the energy of the thermostat, i.e. close to the kinematic limit for the energy of the system. We also chose the energy value $E_2 (E_2 < E_1)$, when the distribution function decreases by an order of magnitude compared to its maximum. When $\varepsilon < E_2$ the amendment δ was supposed equal to zero. In the energy interval $E_2 > \varepsilon > E_1$ it was a linear interpolation between zero and expression (7). Here the correction δ is found for the Boltzmann limit of an ideal gas, since deviations from a grand canonical distribution of the Fermi gas are manifested on the "tails" of the energy spectra when the Fermi distribution coincides with the Boltzmann limit.

- The probability of a microcanonical distribution in the limit of the Boltzmann limit of an ideal gas is

- $$w(\vec{r}, \vec{p}) = C_M \left(1 - \frac{\varepsilon}{U} \right)^M = C_M \exp \left(M \ln \left(1 - \frac{\varepsilon}{MT} \right) \right) \quad , \quad (8)$$

- where ε is the kinetic energy of the system, $U = MT$ is the energy of the thermostat, C_M is the normalization factor [6]. As a result, in the limit of a large number of particles N at $M = \frac{3}{2}N \rightarrow \infty$, expression (8) becomes a grand canonical distribution

- $$w_0(\vec{r}, \vec{p}) = C_M \exp\left(-\frac{\varepsilon}{T}\right)$$

- Thus, on the tails of the energy distributions, using formula (7), we find an amendment for the microcanonical distribution (6), which changes the usual Fermi-Dirac distribution, describing the system well away from the tails of the proton spectrum. Moreover, in formulas (5) - (6) it is taken into account that the energy of the system is recalculated in accordance with the Lorentz transformations. The energy in the distribution (6) is reckoned from the value of the self-consistent mean field with allowance for the surface energy, since the nucleons are "locked" by the mean field.
- In addition to the contribution of (1) to the cross section for the emission of protons from the hot spot, we also took into account the contribution from the fusion of the non-overlapping parts of the colliding nuclei so called "spectators".

A comparison of the calculated energy spectra of protons emitted in the $^{16}\text{O}+^{27}\text{Al} \rightarrow \text{p}+\text{X}$ reaction at an angle of 30° at an ^{16}O ion energy of 207 MeV (~ 12 MeV / nucleon) (curves 1) and 310 MeV (~ 19 MeV / nucleon) (curves 2), with experimental data is shown in Fig. 2. Our calculation describes the data [7] (which have so far been unexplained) with allowance for the introduced amendment for the microcanonical distribution. Without taking this correction into account, the spectra turn out to be more harden (corresponding to this variant of the calculation, the dashed curves 1a and 2a go above the points). The agreement with the experiment is achieved for a non-equilibrium equation of state with a selected compression modulus of $K=210$ MeV and without breaking the agreement with other data.

In Fig. 3 are shown the energy spectra of protons emitted in the $^{14}\text{N}+^{124}\text{Sn} \rightarrow \text{p}+\text{X}$ reaction at angles of 45° (curve 1), 62° (curve 2) and 90° (curve 3) at an ^{14}N ion energy of 32 MeV / nucleon. The calculated curves corresponding to the non-equilibrium equation of state (solid lines) agree with the experimental data [8], in contrast to the dashed lines corresponding to the choice of the equilibrium equation of state, when they go above the experimental points. At the tails, the experimental spectrum is somewhat "cut off," which is apparently due to systematic experimental errors and is not reproduced in the calculation. An amendment for the microcanonical distribution is in a significantly higher region of proton energies (see the previous figure).

Fig.2. $^{16}\text{O} + ^{27}\text{Al}$ 30° (protons)
1-12MeV/nucl., 2-19MeV/nucl.

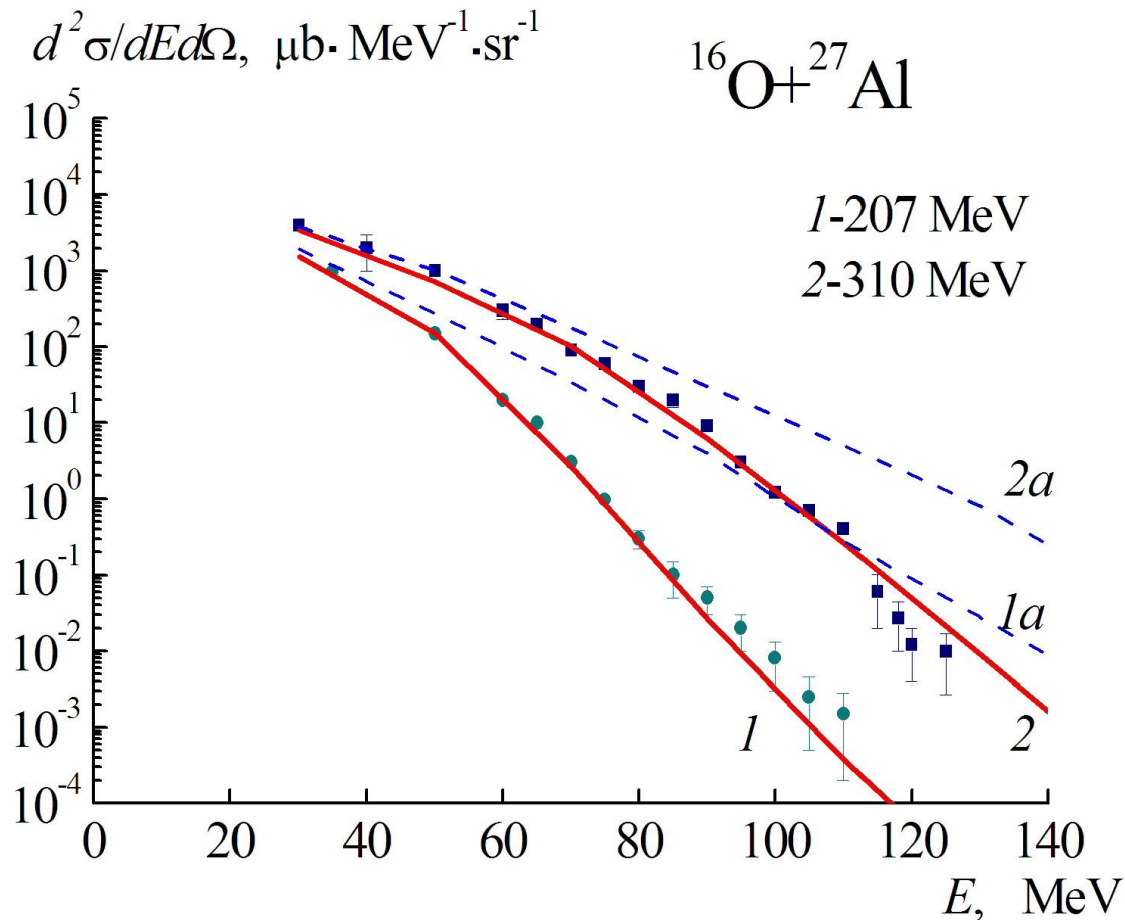


Fig.3. $^{14}\text{N}+^{124}\text{Sn}$ 32 MeV/nucl.
(protons) 1- 45° , 2- 62° , 3- 90°

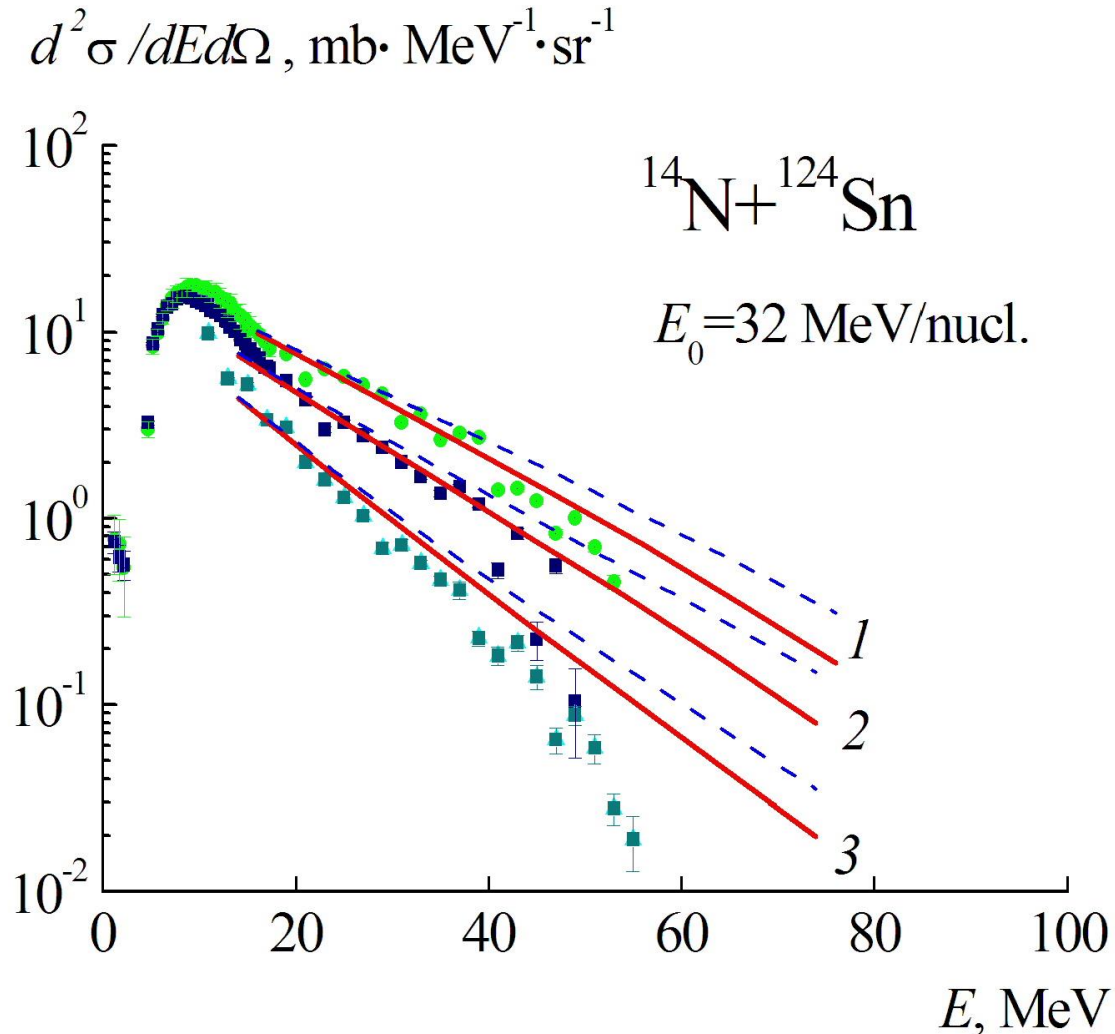


Fig.4. $^{12}\text{C}+^9\text{Be}$ 300MeV/nucl.
(protons) 3,5⁰

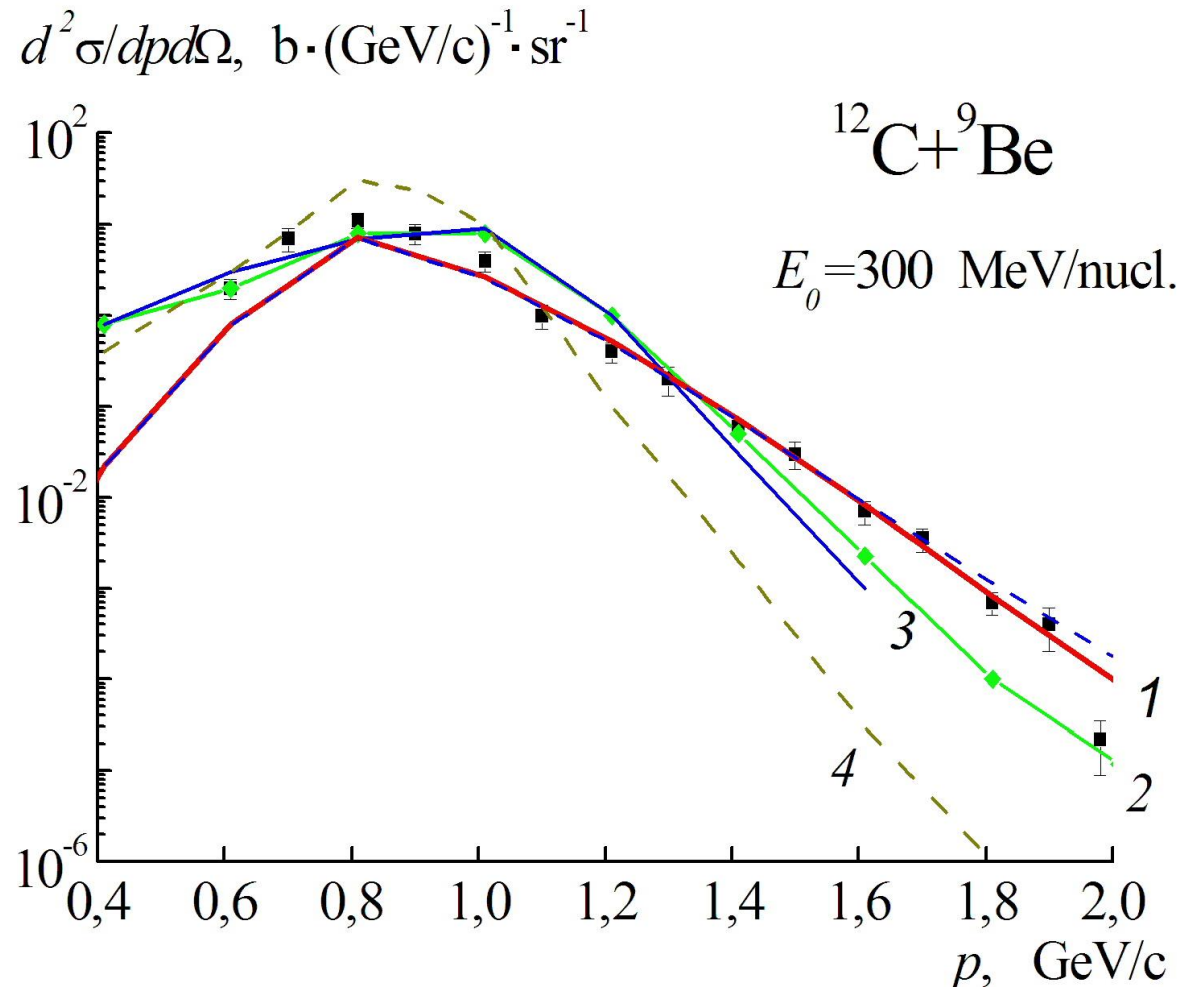


Fig.5. $^{12}\text{C}+^9\text{Be}$ 600 MeV/nucl.
(protons) $3,5^0$

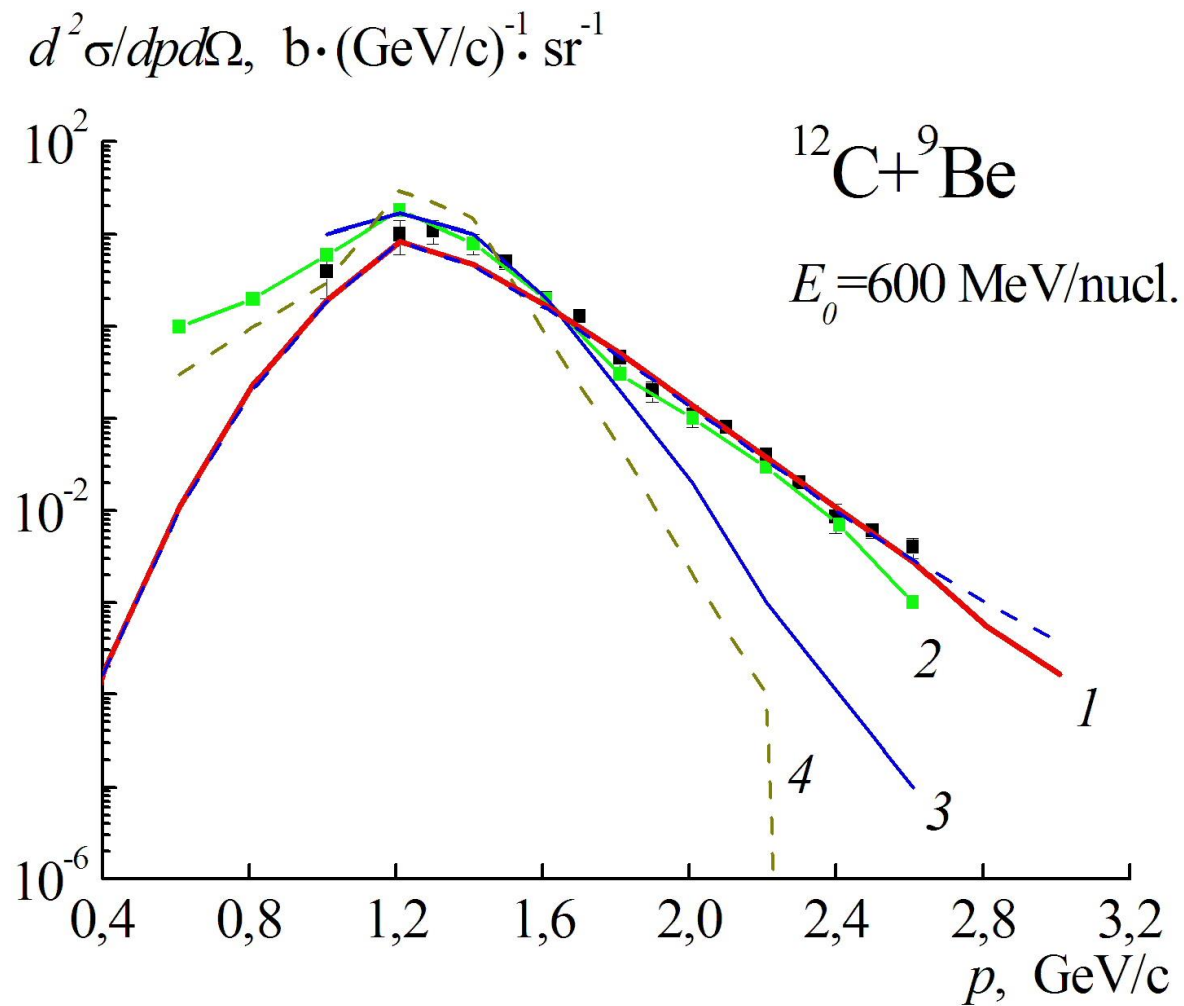


Fig.6. $^{12}\text{C}+^9\text{Be}$ 950 MeV/nucl.
(protons) $3,5^0$

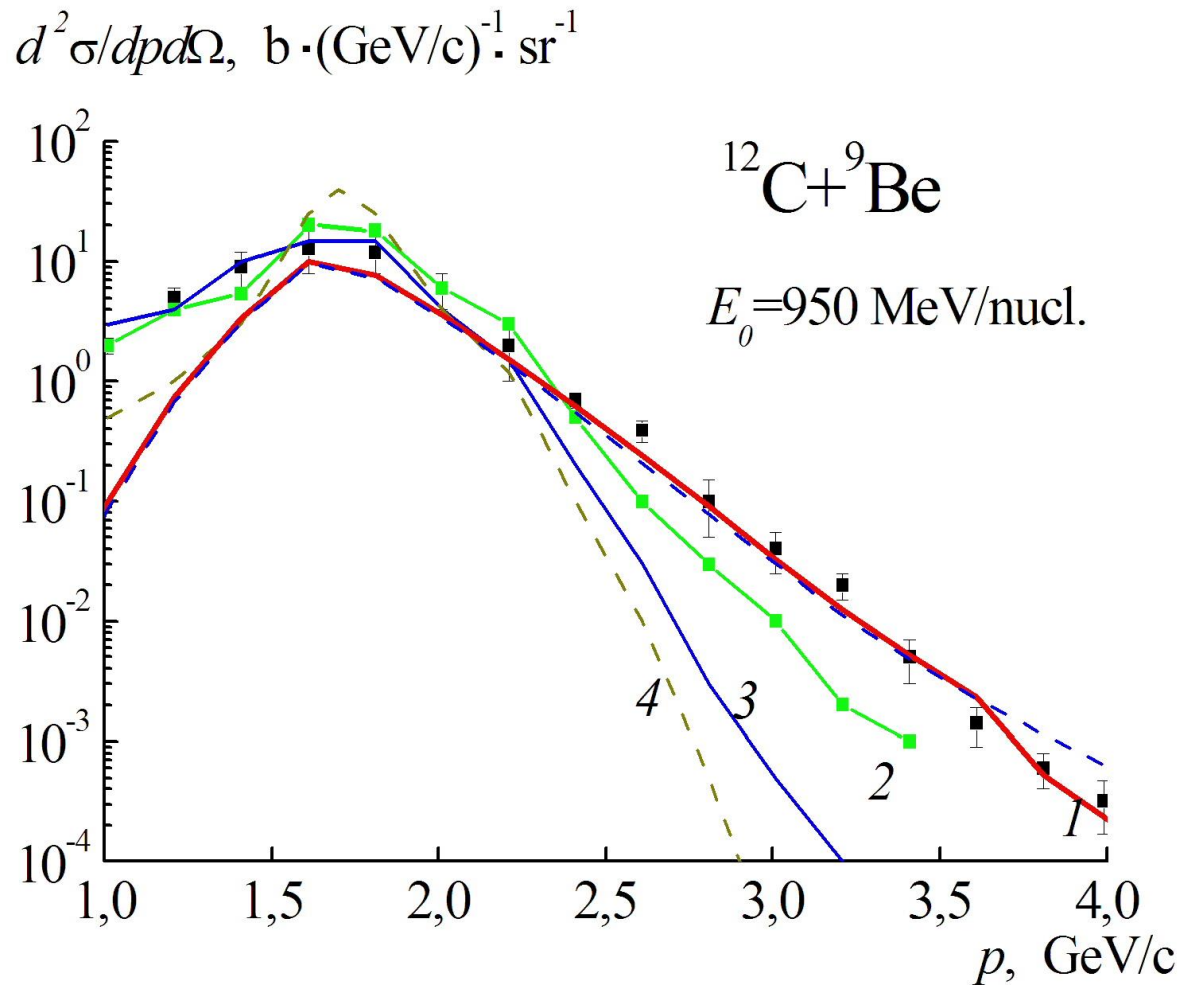
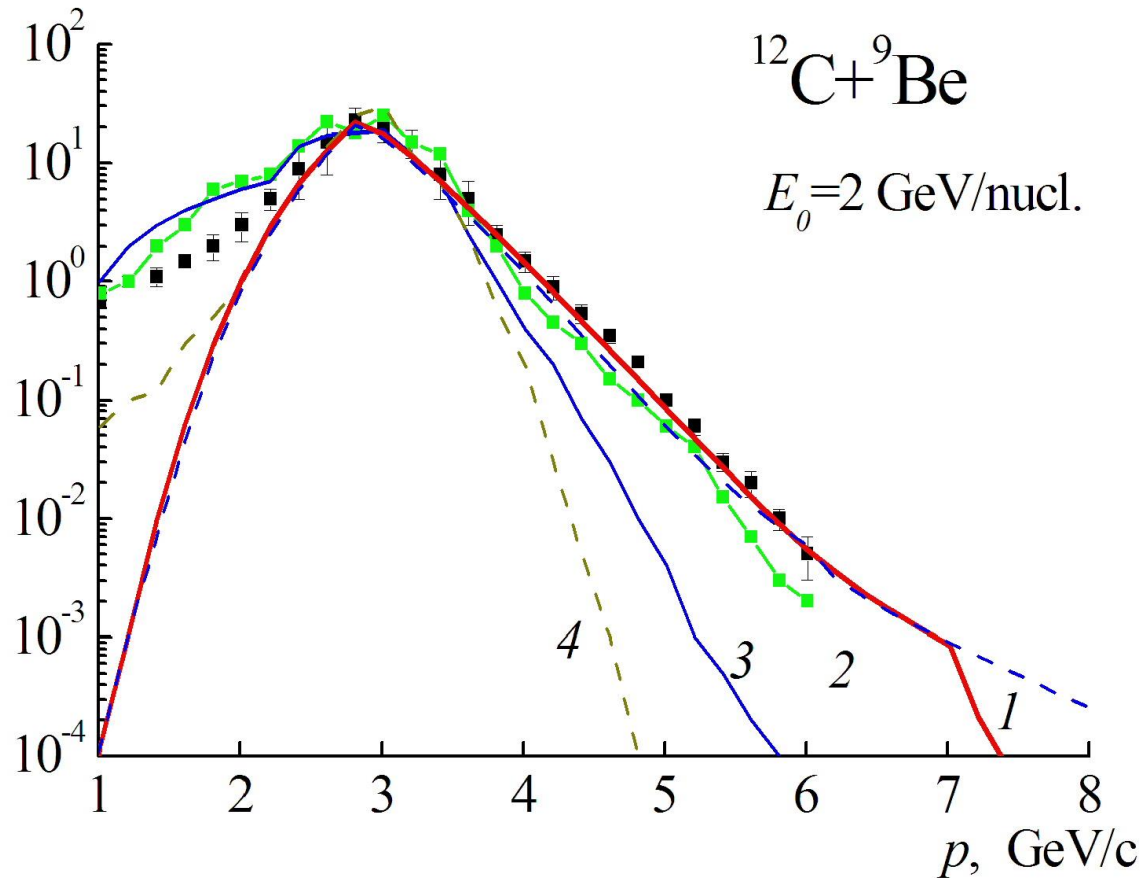


Fig.7. $^{12}\text{C}+^9\text{Be}$ 2 GeV/nucl. (protons) $3,5^0$

$$d^2\sigma/dp d\Omega, \text{ b} \cdot (\text{GeV}/c)^{-1} \cdot \text{sr}^{-1}$$



- In Fig. 4-7 are shown the momentum spectra of protons emitted in the $^{12}\text{C}+^9\text{Be} \rightarrow \text{p}+\text{X}$ reaction at an angle of 3.5° at an ^{12}C ion energy of 300 MeV / nucl., 600 MeV/nucl., 950MeV/nucl.and, 2GeV/nucl. The experimental data [9] are marked by points. The solid curve 1 is our calculation. The dashed curve 1 is our calculation without taking into account an amendment for the microcanonical distribution. Curves 2, 3. 4 are results of calculations for transport codes [9]. Curve 2 corresponds to the cascade model [10], curve 3 corresponds to the transport model of quark-gluon strings [11], curve 4 corresponds to the quantum molecular dynamics (QMD) model built into the GEANT4 package [12]. As can be seen from this figures, in the cumulative region of the spectrum our calculation turned out to be in agreement with the experimental data [9]. The decline in the cross sections by 5 orders of magnitude is reproduced in our approach no worse than in the Monte Carlo transport codes. Some cascade calculations noticeably underestimate these experimental data in the high-momentum region. However, in the region of small momentums, our calculation underestimates the experimental data, which may be due to the contribution from the protons formed as a result of ^{12}C fragmentation. An amendment for the microcanonical distribution (dashed curve 1) appears in this case only at the very tails of the high-momentum distributions of the protons

Conclusion

- Thus, in this paper, the idea of using of a non-equilibrium equation of state in the hydrodynamic approach to describe the high-momentum proton spectra emitted in heavy-ion collisions over a wide energy range has been further developed.
- The experimental shoulder in the cross section for the production of protons in the cumulative region is reproduced by our calculations, and sometimes by cascade models. Perhaps this may be due to the contribution of the rescattering of pions to the cumulative production of protons, considered earlier in [13].

References

- 1. A.T. D'yachenko // Phys. Atom. Nucl. 1994. V. 57. P. 1930.
- 2. A.T. D'yachenko, K.A. Gridnev, W. Greiner // J. Phys. G. Nucl. Part. Phys. 2013. V.40.P.085101.
- 3. A.T. D'yachenko, I.A. Mitropolsky // Bull. Russ. Acad. Sci. Phys. 2017. V. 81. no.12. P.1521.
- 4. A.T. D'yachenko, I.A. Mitropolsky. Construction of the nonequilibrium equation of state for the description of collisions of heavy ions and its application to finding energy spectra of protons and subthreshold pions. The article in the book "In Memory K. A. Gridnev. To the 80th anniversary of his birth. " Gatchina. : NRC "Kurchatov Institute "- PNPI, 2018. P. 63
- 5. A.T. D'yachenko, I.A. Mitropolsky, Yu.G. Sobolev // Proc. VIII Int. Symposium on Exotic Nuclei, Kazan 2016, World Sci. Singapore, 2017. P. 38.
- 6. A.I. Anselm. Fundamentals of statistical physics and thermodynamics. Moscow: Nauka, 1973.
- 7. S.I. Gogolev et al. // Proc. Int. School-Seminar on Heavy Ion Physics. 1993. Dubna. JINR. E7-93-274. V. 2. P. 66.
- 8. V.V. Avdeichikov et al. (CHIC-Collaboration) // Proc. Int. School-Seminar on Heavy Ion Physics. 1993. Dubna. JINR. E7-93-274. V. 2. P. 238.
- 9. B.M. Abramov et al. // Phys. Atom. Nucl. 2015. V.78. P. 373.
- 10. A.V. Dementyev, N.M. Sobolevsky // Nucl. Tracks Radiat. Meas. 1999. V. 30. P. 553.
- 11. S.G. Mashnik et al. // LA-UR-08-2931 (Los Alamos 2008); arXiv.0805.0751 [nucl-th].
- 12. T. Koi et al. // AIP Conf. Proc. 2007. V. 896. P.21.
- 13. M.A. Braun, V.V. Vechernin // Sov. J. Nucl. Phys. 1986. V. 43. P. 1016.

THANK YOU FOR ATTENTION!